

## Hydantoin-based Molecular Photoswitches

David Martínez-López, Meng-Long Yu, Cristina García-Iriepe, Pedro José Campos, Luis Manuel Frutos, James A. Golen, Sivappa Rasapalli, and Diego Sampedro

*J. Org. Chem.*, **Just Accepted Manuscript** • Publication Date (Web): 25 Mar 2015

Downloaded from <http://pubs.acs.org> on March 27, 2015

### Just Accepted

"Just Accepted" manuscripts have been peer-reviewed and accepted for publication. They are posted online prior to technical editing, formatting for publication and author proofing. The American Chemical Society provides "Just Accepted" as a free service to the research community to expedite the dissemination of scientific material as soon as possible after acceptance. "Just Accepted" manuscripts appear in full in PDF format accompanied by an HTML abstract. "Just Accepted" manuscripts have been fully peer reviewed, but should not be considered the official version of record. They are accessible to all readers and citable by the Digital Object Identifier (DOI®). "Just Accepted" is an optional service offered to authors. Therefore, the "Just Accepted" Web site may not include all articles that will be published in the journal. After a manuscript is technically edited and formatted, it will be removed from the "Just Accepted" Web site and published as an ASAP article. Note that technical editing may introduce minor changes to the manuscript text and/or graphics which could affect content, and all legal disclaimers and ethical guidelines that apply to the journal pertain. ACS cannot be held responsible for errors or consequences arising from the use of information contained in these "Just Accepted" manuscripts.



**ACS Publications**  
High quality. High impact.

# Hydantoin-based Molecular Photoswitches

David Martínez-López,<sup>a</sup> Meng-Long Yu,<sup>b</sup> Cristina García-Iriepe,<sup>a,c</sup> Pedro J. Campos,<sup>a</sup>

Luis Manuel Frutos,<sup>c</sup> James A. Golen,<sup>b</sup> Sivappa Rasapalli<sup>b\*</sup> and Diego Sampedro<sup>a\*</sup>

*a)* Departamento de Química, Universidad de La Rioja, Centro de Investigación en Síntesis Química (CISQ), Madre de Dios, 51, 26006 Logroño, Spain.

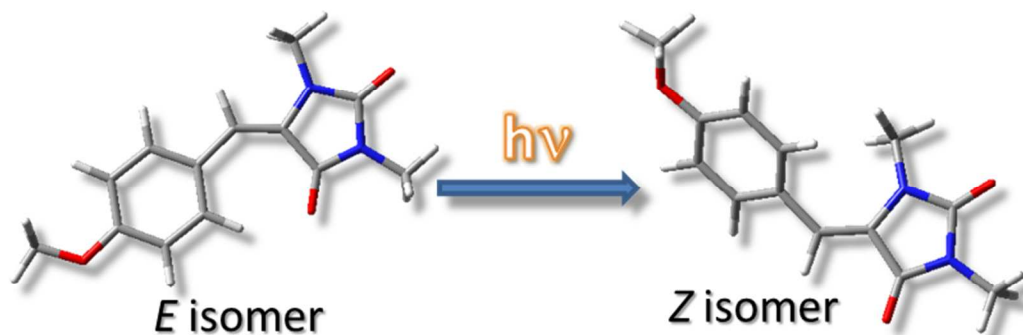
*b)* Department of Chemistry and Biochemistry, University of Massachusetts Dartmouth, North Dartmouth, USA

*c)* Departamento de Química Analítica, Química Física e Ingeniería Química, Universidad de Alcalá, 28871 Alcalá de Henares, Madrid, Spain

diego.sampedro@unirioja.es

srasapalli@umassd.edu

**RECEIVED DATE** (to be automatically inserted after your manuscript is accepted if required according to the journal that you are submitting your paper to)



## Abstract

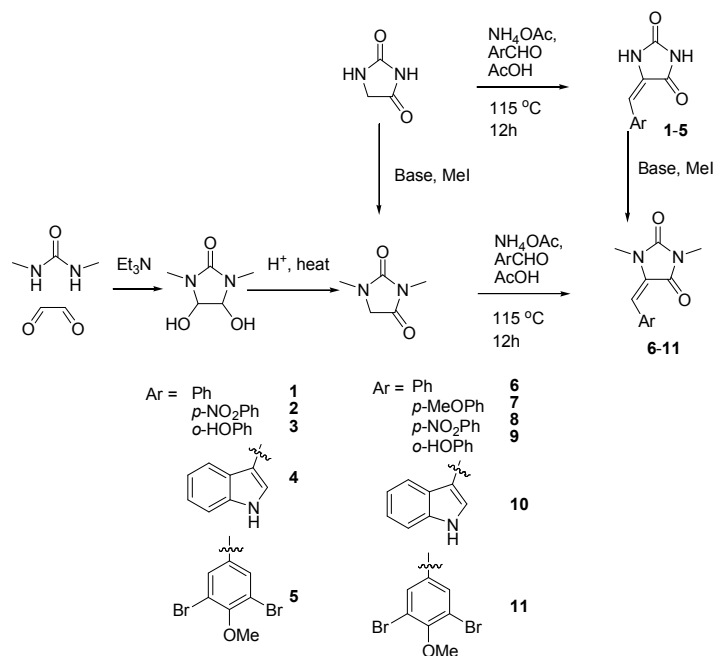
A new family of molecular photoswitches based on arylidenehydantoins is described together with their synthesis, photochemical and photophysical studies. A series of hydantoin derivatives have been prepared as single isomers using a simple and versatile chemistry in good yields. Our studies show that the photostationary states of these compounds can be easily controlled by means of external factors such as the light source or filters. Moreover, the detailed investigations proved that these switches are efficient i.e., they make efficient use of the light energy, high fatigue resistant and very photostable. In some cases, the switches can be completely turned *on* / *off*, a desirable feature for specific applications. A series of theoretical calculations have been also carried out in order to understand the photoisomerization mechanism at the molecular level.

## 1. Introduction.

In recent years, molecular switches and motors<sup>1,2</sup> have been used in very different applications with great success. Specifically, photoactive molecular switches have allowed to control diverse properties from the shape of crystals<sup>3</sup> to protein engineering,<sup>4</sup> activity of biological systems<sup>5</sup> or orientation in liquid-crystalline polymers.<sup>6</sup> Modifying the structure of the switch and, thereby, the properties of complex systems by light as the external stimulus has some advantages:<sup>1</sup> 1) selected wavelengths can be used to minimize the damaging effect of light in the system; 2) a high degree of spatial and temporal resolution can be obtained; 3) no waste products are obtained after the photon absorption. In spite of the increasing number of promising applications of photoswitches, most of the compounds employed to photocontrol the properties of complex systems share a common set of basic chemical properties. The available molecular photoswitches can be classified in two main classes depending on the photochemical process that allows the switch between the two isomeric forms. Type I: Compounds that can photoisomerize between closed and open forms. Among this type of photoswitches the dimethyldihydropyrene (DHP)/cyclophanediene (CPD) system,<sup>7-10</sup> diarylethenes<sup>11-13</sup> and spiropyranes<sup>14-17</sup> have been developed. Type II: Compounds that can undergo the isomerization of a

double bond as in the *E/Z* photochemical switches. Of the several families of *E/Z* photochemical switches, azobenzenes<sup>18-20</sup> have been extensively used due to their stability, adequate photophysical properties, and the ease of synthesis and derivatization. Besides, overcrowded alkenes<sup>21</sup> have been applied as photoswitches to control diverse properties, but also as frameworks in the preparation of molecular motors.<sup>22</sup> Several other switches have been reported<sup>23</sup> including retinal-based switches,<sup>24-29</sup> green fluorescence protein (GFP) analogues<sup>30,31</sup> and hemithioindigos.<sup>32-38</sup> Although numerous efforts have been made in order to generalise the concept of molecular photoswitch at the theoretical level,<sup>39</sup> the preparation and photochemical study of new families of switches seems critical for enabling more complex and specific applications. Towards this direction, we have been intrigued by the possibility of developing a new family of photoswitches based on 5-arylidenehydantoins.

5-Arylidenehydantoins (5-AHTs) belong to a novel family of (GFP) analogues, where the imidazoline unit is replaced by an imidazolinone moiety.<sup>23</sup> The first synthesis of 5-AHT, from the reaction of phenylpropionic acid and urea, was reported in 1899.<sup>40</sup> Some years later, Wheeler and Hoffman described a more effective method to prepare 5-AHT from the condensation of hydantoin and benzaldehyde in acidic solution.<sup>41</sup> The applications of 5-AHTs are mainly focused on their biological activities. To date, multiple functions such as anticancer, antibiotic, and antagonistic properties, have been reported.<sup>42</sup> However, there are only scant reports about the study of their photochemical properties. In this respect, it was demonstrated<sup>43</sup> the application of 5-AHT in the cosmetics industry as an excellent UV absorbent. Due to the structural similarity of 5-AHTs with the GFP-like molecular photoswitches previously reported,<sup>44</sup> the capability of *Z/E* photoisomerization<sup>45-47</sup> and their superb thermal and photochemical stability, we decided to explore their behavior as molecular photoswitches. Accordingly, we have carried out detailed investigations, and herein we report the synthesis, photochemistry and theoretical study of a library of molecular photoswitches based on the 5-arylidenehydantoin structure.



Scheme 1. Synthesis of compounds 1-11.

## 2. Results and Discussion.

The new series of molecular photoswitches was synthesized according to Scheme 1. Thus, 5-arylidenehydantoin derivatives **1-5** were synthesized from the condensation of hydantoin and different aromatic aldehydes in acetic acid/ammonium acetate mixture in good yields (70-80%, see Supporting Information for synthetic details), according to a previously reported method.<sup>48</sup> The disubstituted 1,3-dimethyl-5-arylidenehydantoin derivatives **6-11** were obtained in two different ways. In the first method, *via* the 5-arylidenehydantoin derivatives previously synthesized from aldehydes and hydantoin condensation as described above, were subjected to bis-methylation with excess of methyl iodide to produce the 1,3-dimethyl-5-arylidenehydantoin series. However, this method had limitations regarding to purification and the presence of other potential nucleophilic functionalities. So, we resorted to an alternative method in order to solve this problem by accessing the dialkylated precursor, *i.e.*, 1,3-dimethylhydantoin obtained either *via* de novo synthesis or through bis-methylation of hydantoin. Thus, treatment of glyoxal with *N, N'*-dimethylurea, followed by pinacol rearrangement delivered clean formation of 1,3-dimethylhydantoin. The condensation of this compound with various aldehydes afforded the 1,3-dimethyl-5-arylidenehydantoin derivatives as final products. Under both reaction conditions, the *E* isomer was found to be the

only isomer. In any case, the *Z* isomer was not detected by NMR. The configuration of the obtained products was in turn confirmed by the X-ray diffraction data for **7** (Figure 1).

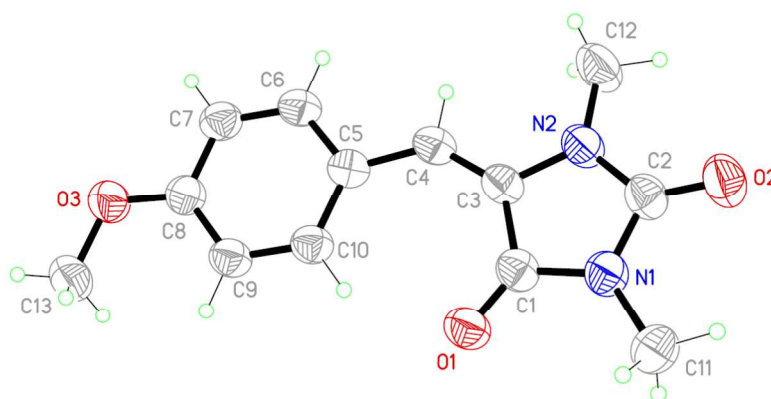


**Figure 1:** Solid state structure of *E*-**7** with thermal ellipsoids shown at 50% probability.

All the hydantoin based compounds synthesized share a typical UV absorption spectrum as exemplified in Figure 2 by the spectrum of **7** in CH<sub>2</sub>Cl<sub>2</sub> : MeOH (1:1) . In all the cases, a strong absorption band between 320 and 370 nm was found for **1-11** (see Table 1). This is relevant as low-energy wavelengths could be used to promote the photoisomerization which, in turn, confers a wider applicability to these switches. Also, the solvent effect was investigated by recording the UV spectra in acetonitrile, chloroform or DMSO. No significant changes were detected in the spectra for the tested solvents. The effect of dimethylation of the hydantoin moiety has a minor effect in the absorption spectra for these compounds. A small shift of 10-15 nm was found when comparing the 5-arylidenehydantoin **1-5** with their equivalents 1,3-dimethyl-5-arylidenehydantoin **6-11**. However, the two series of compounds show different solubility features, as **1-5** are only soluble in CH<sub>2</sub>Cl<sub>2</sub> : MeOH mixtures and DMSO while **6-11** are very soluble in common organic solvents. Thus, different experimental conditions are available for these switches while the absorption properties remain similar.

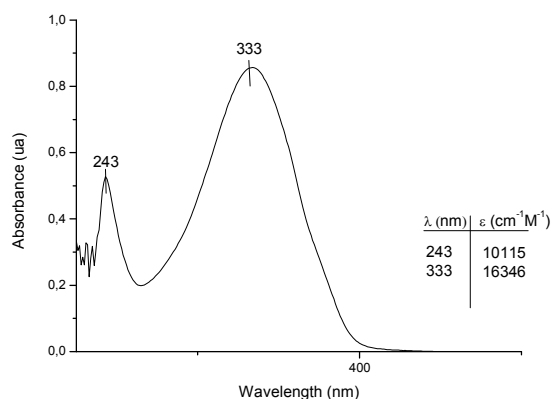


**Figure 2.** UV-Vis spectrum of **7**.

Irradiation of the compounds **1-11** was performed with a 400 W medium-pressure Hg lamp through a Pyrex filter (to avoid light with wavelength below 290 nm) in an immersion well or in a Pyrex NMR tube. The progress of the reaction was easily monitored by <sup>1</sup>H-NMR and TLC as the *Z* and *E* isomers for every compound show clearly different chemical shifts (specially the vinyl hydrogen) and *R<sub>f</sub>* values. For instance, the vinyl hydrogen of **1** appears in <sup>1</sup>H-NMR as two distinct singlets at 6.41 ppm (*E*-**1**) and 6.32 ppm (*Z*-**1**, see Supporting Information). In the case of **5**, these two signals appear at 5.59 ppm (*E*-**5**) and 6.33 ppm (*Z*-**5**). Thus, photoisomerization could be easily and quantitatively followed by NMR. Irradiation was maintained until the photostationary state (PSS) was reached. Typically, this required *ca.* 45 min in a Pyrex tube. The composition of the PSS under these conditions for compounds **1-11** is shown in Table 1.

Interestingly, no decomposition was observed by NMR in the course of the photoisomerization even after several hours of continued irradiation once the PSS was reached. This is relevant as potential applications of these switches that imply long periods of irradiation could be envisaged. Thus, photostability is a valuable feature for any photoswitch. We have probed the stability of compounds **1-11** further in two different ways. First, all the compounds were subjected to further irradiation for at least 4 hours after the PSS was reached (*ca.* 45 min). In no case decomposition was observed by NMR. It should be noted that during this time both isomers are continuously absorbing and reacting in a

dynamic equilibrium. As a second measure of photostability and capability of performing several cycles without decomposition, several photoisomerization cycles were performed for compounds **2** and **7** as representative examples (Figure 3). For instance, a solution of *E*-**7** was irradiated using light of 375 and 300 nm alternatively and the isomerization was followed by the absorbance at 333 nm (maximum absorption wavelength for *E*-**7**). Both isomers could be interconverted for several cycles without apparent decomposition. Therefore, those two experiments indicate the high photostability and fatigue resistance of these switches which constitutes a requisite for practical applications.



**Table 1.** Absorption maximum and photostationary state (PSS) for **1-11** at different irradiation wavelengths in CH<sub>2</sub>Cl<sub>2</sub> : MeOH (1:1).

Compound	$\lambda_{\text{max}}$ <sup>[a]</sup>	PSS ( <i>E</i> : <i>Z</i> ) <sup>[b]</sup>	PSS( <i>E</i> : <i>Z</i> ) <sup>[c]</sup>
1	317	100:0 <sup>[d]</sup>	95:5
2	353	64:36	53:47
3	340	86:14	48:52
4	367	89:11	22:78
5	321	0:100	19:81
6	309	100:0 <sup>[d]</sup>	
7	333	5:95	35:65
8	339	69:31	
9	326	88:12	
10	373	45:55	
11	316	100:0 <sup>[d]</sup>	

[a] Value in nm for *E* isomer [b] Pyrex-filtered medium-pressure Hg lamp. [c] Photoreactor (350 nm).

[d] Photoisomerization takes place in quartz, see text.

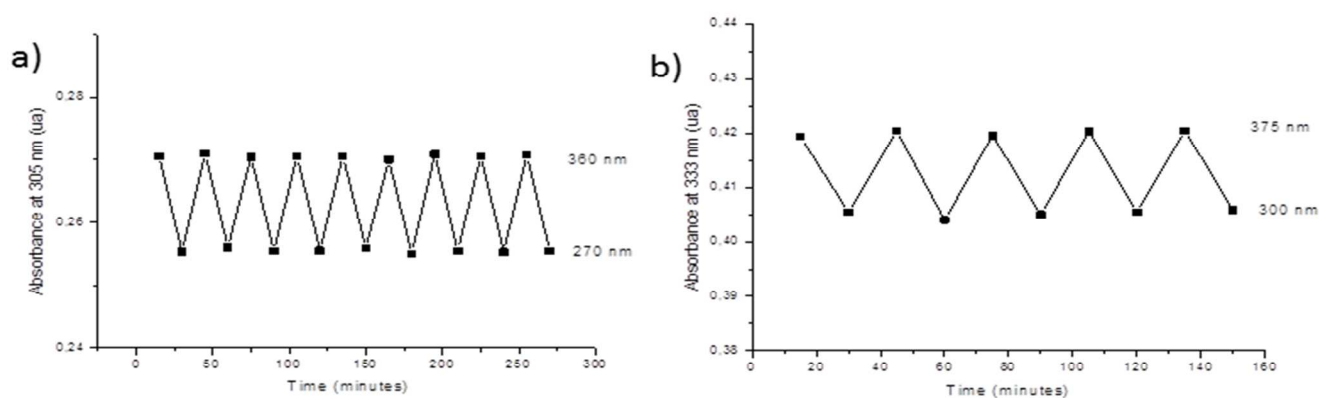


**Figure 3.** Photoisomerization cycles for a) **2** and b) **7**.

In addition, the photoisomerization kinetics was studied for *E*-7 using  $^1\text{H}$ -NMR to determine the relative concentrations at short irradiation time intervals (Figure 4). From the first points, when the composition of the mixture is mainly the *E* isomer and the absorption of the *Z* isomer is minimized, a kinetic constant of  $2.57\text{ s}^{-1}$  was obtained. Thus we concluded that, under these conditions, a fast photoisomerization takes place.

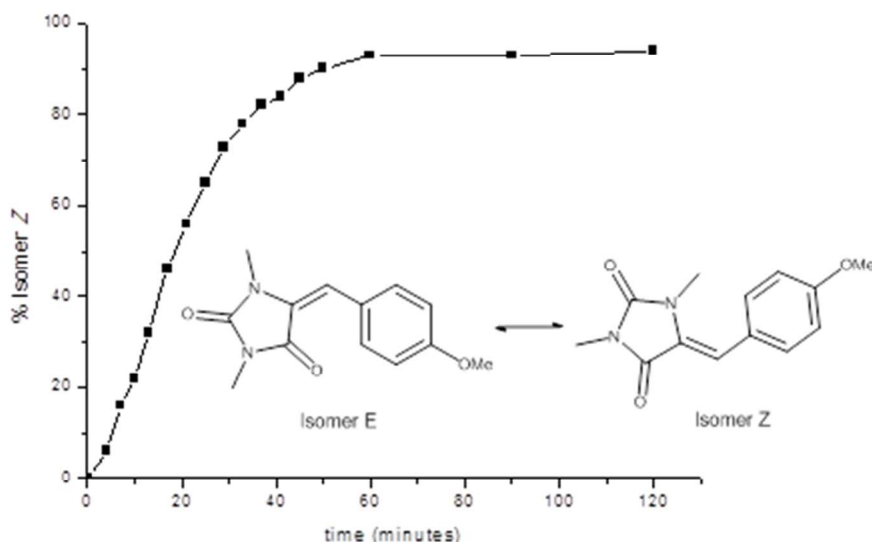


**Figure 4.** Composition of the mixture during irradiation of *E*-7 at different time intervals.

As shown in Table 1, the PSS ratio is strongly dependent on the aryl substituent as different *E*:*Z* ratios were obtained. The composition of the PSS is affected by the relative absorption of the isomers, their relative stability and the topology of the potential energy surfaces. In turn, all these factors could be different for every compound in Table 1. Also, the PSS depends on the quantum yields of the forward (*E* to *Z*) and backward reactions (*Z* to *E*). In turn, these quantum yields are affected by the relative absorption of both isomers and the shape of the potential energy surfaces. Thus, providing a general quantitative rationale of the PSS is a complex issue. However, some qualitative indications of the relevance of those factors could be obtained. As the relative absorption of the *E* and the *Z* isomers is clearly dependent upon the irradiation source, a different PSS could be obtained for the switches under different irradiation conditions (see below). In this case, it is relevant to check as to which isomer

absorbs light preferentially at a specific light source or wavelength. Also, the topology of the potential energy surface is relevant in order to determine the composition of the PSS. For these compounds, the decay to the ground state after excited state relaxation implies a geometry twisted *ca.* 90° (see the computational paragraphs below). However, this torsion angle is expected to be affected by the electronic nature of the substituents as it has been found for other *E* / *Z* photoswitches.<sup>23</sup> A complete exploration of the effect of substitution (in both the absorption spectrum and the potential energy surface topology) is beyond the scope of this paper. However, some conclusions can be derived from the analysis of Table 1. For instance, in most cases the thermally stable isomer *E* is also the main isomer in the PSS when a Pyrex filter is used (see **2-4**, **8-9**, Table 1). This is probably due to the slightly stronger absorption of the *E* isomers under these irradiation conditions (see Supporting Information). A different situation was found for **1**, **6** and **11** as these compounds do not photoisomerize under the same conditions. However, for all three compounds, photoisomerization can take place by simply removing the filter and using a quartz-filtered light. In these cases, the relative absorption of both isomers changes when the irradiation source is modified. Under these different conditions, the PSS is 79:21 for **1**, 61:39 for **6** and 54:46 for **11**. Isolation of the photoproduct **1-Z** by column chromatography allowed for the recording of the UV spectrum (see Figure 5).

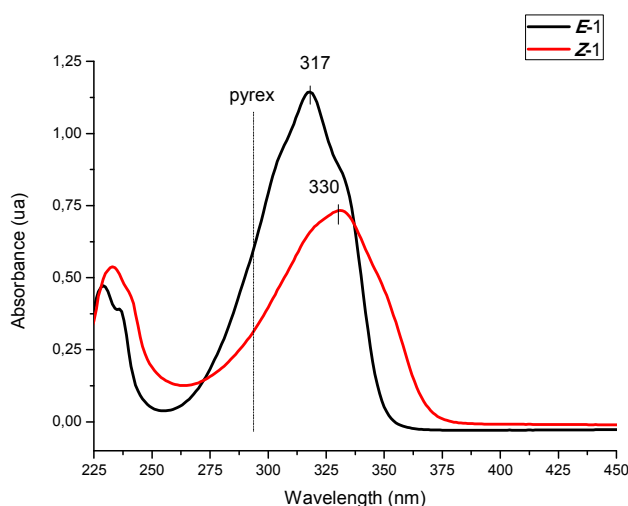


**Figure 5.** UV-Vis spectrum of *E*-**1** and *Z*-**1**.

As it can be seen, the photoisomer features a tail at longer wavelengths causing a higher absorption when a Pyrex filter is used. Thus, although the photoisomerization can take place, the back reaction from the *Z* isomer to the thermally stable *E* isomer is faster under these conditions. However, when a quartz-filtered light is used, the whole band of the *E* isomer is included in the absorption window and the competitive back-reaction is not that effective, allowing for the observed PSS. We checked this effect by following the conversion of a pure *E*-1 sample until the PSS was reached using  $^1\text{H}$ -NMR (Figure 6).

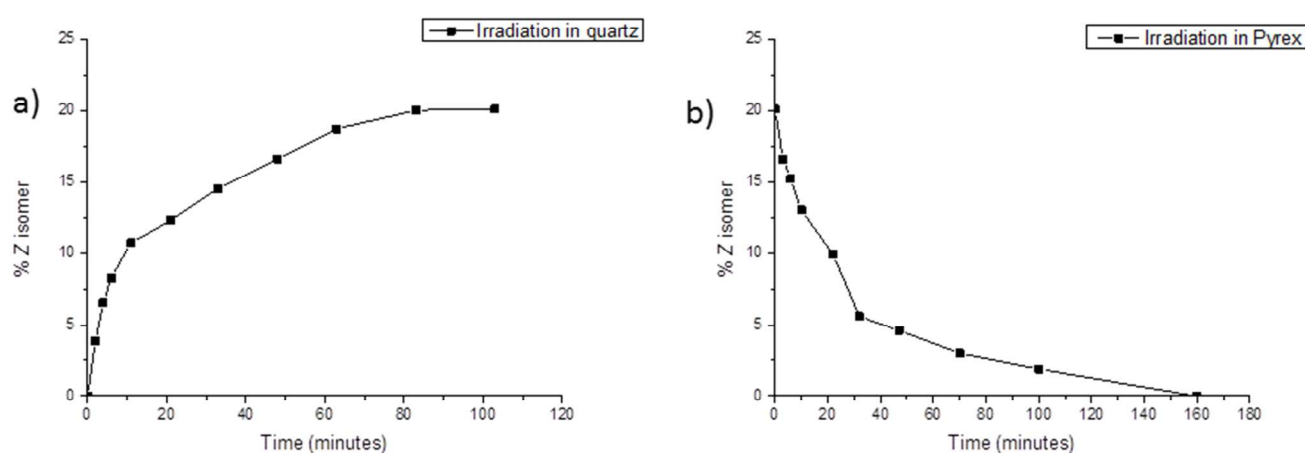


**Figure 6.** Composition of the mixture under irradiation of **1** using a) quartz and b) Pyrex filters.

As it can be seen, using a quartz filter, the irradiation continuously induces the photoisomerization of **1** until a mixture of isomers in a 79:21 ratio is reached (Figure 6, a). Subsequent irradiation of the same solution through a Pyrex filter leads to the starting situation of pure *E*-isomer (Figure 6, b). Alternative irradiation of the same sample of **1** using Pyrex and quartz as filters during several cycles allowed the formation of different mixtures with Pyrex and quartz with no observable decomposition (Figure 7). We anticipate that this stability would allow to easily alter the PSS by an external agent as is the use of different types of filters. In addition, this result proves the high fatigue resistance of the hydantoin based switches under relatively long irradiation times even using a high-energy irradiation source. The same behaviour was also found for **6** and **11**.

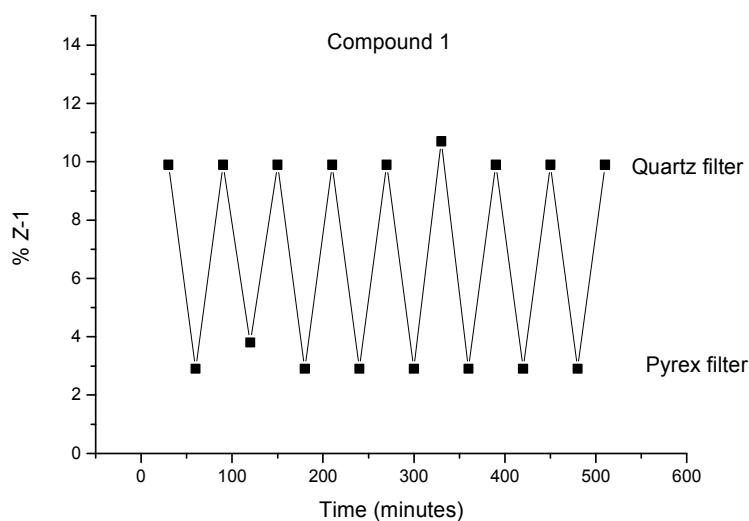


**Figure 7.** Photoisomerization cycles for **1**.

Some relevant results were also found for **5** and **7**. In these two cases, the *Z* isomer was not only the main product in the PSS, but it was obtained almost quantitatively. This implies that starting from the pure *E*-**5** obtained directly from synthesis, only the photoisomer *Z*-**5** was detected by NMR after its irradiation. This excellent feature allows for a complete change in the switch position, that is, the switch can be completely changed from the *off* state to the *on* state. Although this would be highly desirable for photoswitches, such a complete change is not common at all. In fact, most systems reported in the literature only allow the modification of the PSS but not a complete change in the switch state.<sup>2</sup>

In order to generalize the effect of the light source on the process, we also tested the photoisomerization using a photoreactor with emission centred at 350 nm (14 lamps x 8W/lamp). For this, we chose compounds **2-4** as they showed neat absorptions in the 350 nm region (see Supporting Information, Figure S1), together with **1**, **5** and **7** to check the generality of the effect. Results are shown in Table 1. For **2-4**, the use of this light source causes a different PSS enriched in the *Z* isomer (see Figures S2-S4). Again, this fact attests additional practical flexibility of these systems as the PSS can also be modified easily with an external agent.

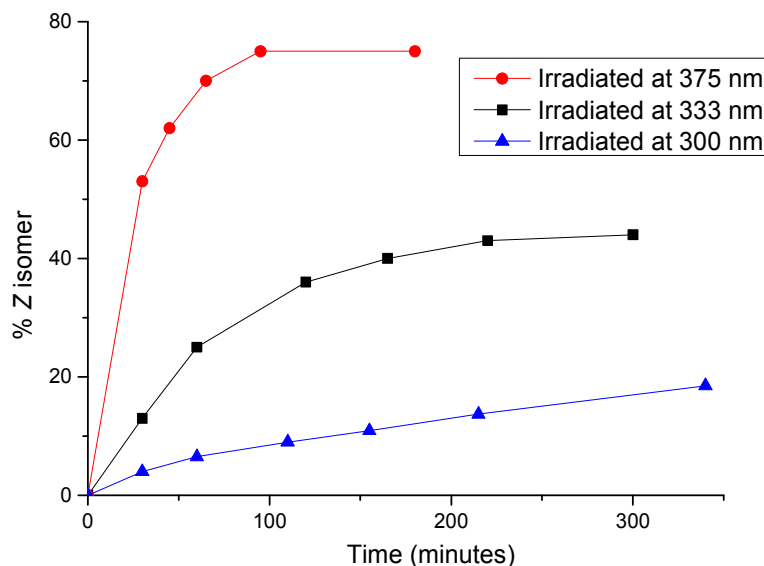
Furthermore, the effect of monochromatic light in the photoisomerization process was studied. For this study we chose **5** and **7**, as the *Z* isomer was found almost exclusively in the PSS. The comparative UV spectra for the *E* and *Z* isomers of **5** and **7** are shown in Figures S5 and S6. Regarding **5**, the thermal *E* isomer featured a stronger absorption along the complete range of wavelengths. Thus, its irradiation would lead in any case to the *Z* isomer as the main isomer in the PSS. However, in the case of **7**, both isomers showed a slight displacement between their absorption maxima. Although small, this difference could be enough to displace the PSS. We tested this fact by irradiating at three different wavelengths, namely 300, 333 and 375 nm. Results are shown in Table 2.

**Table 2.** Irradiation of **7** at selected wavelengths.

$\lambda$ (nm)	<i>E</i> isomer (%)	<i>Z</i> isomer (%)
300	78	22
333	55	45
375	25	75

Hence, it can be concluded that small variations in the irradiation wavelength lead to significant changes in the PSS. Specifically for **7**, changing the irradiation wavelength from 300 nm to 375 nm may change the main isomer in the PSS from the *E* isomer to the *Z* isomer. This fact shows the enormous versatility of this new family of molecular switches which can be interchanged between both states with ease. In order to further clarify the effect of monochromatic light, we followed the irradiation of fresh samples of pure **E-7** using light of varied wavelengths *i.e.*, 300, 333 and 375 nm (Figure 8). As can be seen, the PSS is different for each wavelength, 22%, 45% and 75% of the *Z* isomer, respectively (Table 2). Also, using light of 375 nm the PSS (75% in *Z* isomer) is reached faster than using light of 300 or 333 nm. It should be noted that the absorption at 333 nm is higher for both isomers (see Figure S6). These facts can be explained by the relative absorption of both isomers at each wavelength. As both the forward ( $E \rightarrow Z$ ) and reverse reaction ( $Z \rightarrow E$ ) take place the kinetics and the PSS are affected by the

1 difference in absorption of both isomers. In this specific case, the absorption difference is bigger at 375  
2 nm which explains the reported results.  
3  
4  
5  
6



27 **Figure 8.** Composition of the mixture when irradiating *E-7* using monochromatic light.  
28  
29  
30  
31

32 Having established the feasibility of the photoisomerization, in order to determine the  
33 proficiency of these compounds as molecular photoswitches, their relative efficiency in relation with  
34 alternative deactivation pathways needed to be evaluated. A common competitive pathway with the  
35 photoisomerization is the fluorescence emission. Thus, we checked the luminescent properties of **2**, **7**  
36 and **8** as representative examples (see Figure 9 and Figures S7 and S8).  
37  
38  
39  
40  
41  
42  
43  
44  
45  
46  
47  
48  
49  
50  
51  
52  
53  
54  
55  
56  
57  
58  
59  
60

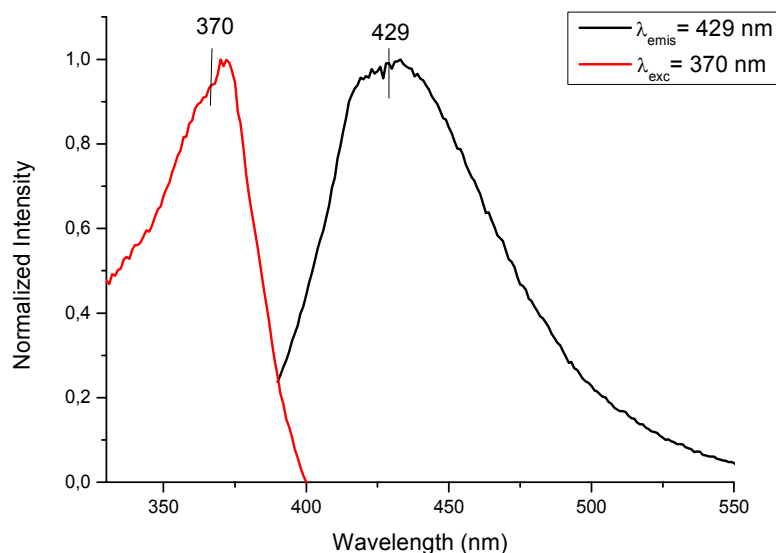


**Figure 9.** Excitation and emission spectra for **7**.

A similar emission pattern was found for **2**, **7** and **8**, in all cases, a single emission band was found. For **7**, the emission is located at 429 nm, while for **2** and **8** the band is centred at *ca.* 530 nm. A slightly bigger Stokes shift was found in the case of **8** (150 nm). However, in all cases, the emission quantum yield was below the apparatus threshold which, in our case, allowed to set an upper limit of  $\Phi_{\text{em}} < 0.1\%$ .<sup>49</sup> Thus, we proved that the radiative deactivation of the excited state is not a competitive pathway. To quantify the efficiency of the photoisomerization, we measured the reaction quantum yield for **3** and **7** as representative examples. Using *trans*-azobenzene as actinometer<sup>50</sup> and measuring the conversion of the *E* into the *Z* isomer at short times we obtained a  $\Phi$  of  $15\% \pm 1\%$  for irradiation at 334 nm for **3** and  $16\% \pm 1\%$  for **7**. Although these values are not as high as some of the recently reported,<sup>44</sup> they do confirm that this new family of compounds is quite efficient and promising. Finally, the thermal reverse-reaction of the *Z* to *E* isomer was also measured for different compounds as this could be relevant for the potential applications. While thermal stability of the photogenerated isomer is usually desirable, for some applications a fast thermal back-reaction is required.<sup>51</sup> Thus, we studied the thermal isomerization of the *Z* isomer for **4**, **5** and **7**. A slow back-reaction (1 week) was



found for **4** at 70°C but not for **5** or **7**. Increasing the temperature to 100°C lead to faster isomerization for **4** and some degree of isomerization was found for **7** (22 days), while no back-reaction was found for **5**. In this case, slow thermal degradation was found by NMR upon heating at 120°C (two days). Thus, in general, these compounds proved to be quite stable to the thermal back reaction. The different time scales found can be attributed to the electronic influence of the substituents on the aryl moiety that affect the transition structure of the isomerization.

In order to understand the photophysics and photochemistry of the reported photoswitches, a computational study using the MS-CASSCF//CASPT2 methodology<sup>52,53</sup> was performed on **7**, as a representative example (see Supporting Information for Computational Details). First, the structures of the *E* and *Z* isomers were optimized in the ground state at the MP2/6-31G\* level of theory (Figure 10). While the *E* isomer minimum is planar, the *Z* isomer is slightly twisted due to the steric hindrance between the methyl and phenyl group. Indeed, the phenyl group is much more twisted *ca.* 47 ° (dihedral C5 C4 C3 C2) compared to the *E* isomer.

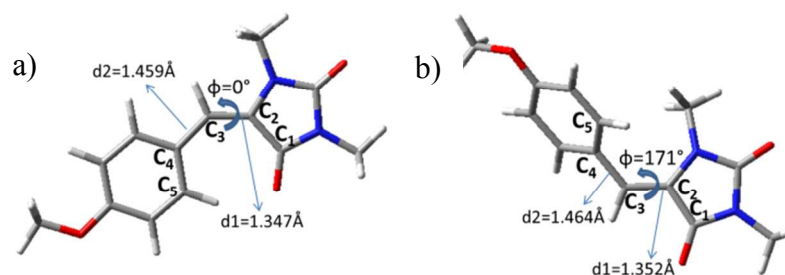


**Figure 10.** Structure of the ground state minima for the *E* (a) and the *Z* (b) isomers of compound **7**.

(C1 C2 C3 C4 dihedral is defined as  $\phi$ ).

The absorption spectrum for both isomers and the photoisomerization mechanism of the *E* isomer (thermally stable) were calculated with the MS-CASPT2//SA-CASSCF methodology using a 6-31G\* basis set. For the absorption spectra simulation we chose six  $\pi$  orbitals (all the  $\pi$  backbone), the corresponding  $\pi^*$  orbitals and two  $n$  orbitals (one of the nitrogen atom and other one of the carbonyl moiety closer to the chromophore). Then, the active space was reduced by removing those orbitals with

almost 2.0 or 0.0 occupation numbers to calculate the minimum energy path, including 5  $\pi$  orbitals, the corresponding  $\pi^*$  orbitals and one n orbital of the carbonyl moiety (see Supporting Information for complete details), obtaining the same energetics as in the large active space.

Both isomers exhibited similar absorption spectra, as experimentally observed. The first excited state ( $S_1$ ) is an optically bright one (see Tables 3) whereas the second ( $S_2$ ) and the third ( $S_3$ ) excited states are dark states (see Tables 3). The electronic transition nature of  $S_1$  is described mainly by the excitation of one electron from the bonding  $\pi$  to the antibonding  $\pi^*$  orbital of the central  $C_2=C_3$  bond, selective of photoisomerization (see Figure S9).  $S_2$  and  $S_4$  are also described by an excitation (single and double, respectively) from one bonding  $\pi$  to one antibonding  $\pi^*$  orbital, whereas the  $S_0 \rightarrow S_3$  electronic transition is due to the mono-excitation from an n orbital to an antibonding  $\pi^*$  orbital. The effect of the solvent was modelled by applying the polarizable continuum model (PCM) obtaining similar results as those found for the gas phase (Table 3).

**Table 3.** Experimental (chloroform), CASPT2 vertical transitions energies (gas phase and in chloroform), electronic nature and oscillator strengths (f) for each transition of **7**.

Isomer	Band eV (nm)	State	$E_{CASPT2}^{Vacuum}$ eV (nm)	$E_{CASPT2}^{PCM}$ eV (nm)	Transition	f	Relative f
<i>E</i>	3.72 (333)	S <sub>1</sub>	3.72 (333)	3.69 (336)	( $\pi, \pi^*$ )	0.4982	0.5609
		S <sub>2</sub>	4.64 (267)	4.65 (266)	( $\pi, \pi^*$ )	0.0009	0.0010
		S <sub>3</sub>	4.78 (259)	4.86 (255)	( $n, \pi^*$ )	0.0006	0.0007
		S <sub>4</sub>	5.81 (213)	5.75 (215)	( $\pi, \pi^*$ ) <sup>2</sup> , ( $\pi, \pi^*$ )	0.3885	0.4374
<i>Z</i>	3.83 (324)	S <sub>1</sub>	3.59 (345)	3.56 (347)	( $\pi, \pi^*$ )	0.4910	0.5342
		S <sub>2</sub>	4.53 (274)	4.54 (273)	( $\pi, \pi^*$ )	0.0209	0.0227
		S <sub>3</sub>	4.74 (262)	4.84 (256)	( $n, \pi^*$ )	0.0078	0.0085
		S <sub>4</sub>	6.00 (207)	5.94 (209)	( $\pi, \pi^*$ ) <sup>2</sup> , ( $\pi, \pi^*$ )	0.3995	0.4346

Finally, the photochemistry of the thermal stable *E* isomer was studied as detailed below. As per our calculations, after excitation to the optically bright state, S<sub>1</sub>, from the Franck–Condon structure, the system relaxes along the stretching coordinate in a first step, leading to a bond length alternation of the single and double bonds (d1 from 1.347 Å to 1.432 Å and d2 from 1.459 Å to 1.402 Å, see Figure 10 for d1 and d2 definition). Following the minimum energy path, the system relaxes on the first excited state

rotating along the formal double bond *ca.* 90 degrees. At this point, the energy gap between  $S_1$  and  $S_0$  is *ca.* 20 kcal/mol at the CASPT2 level of theory and the coupling between both states is large (Figure 11).

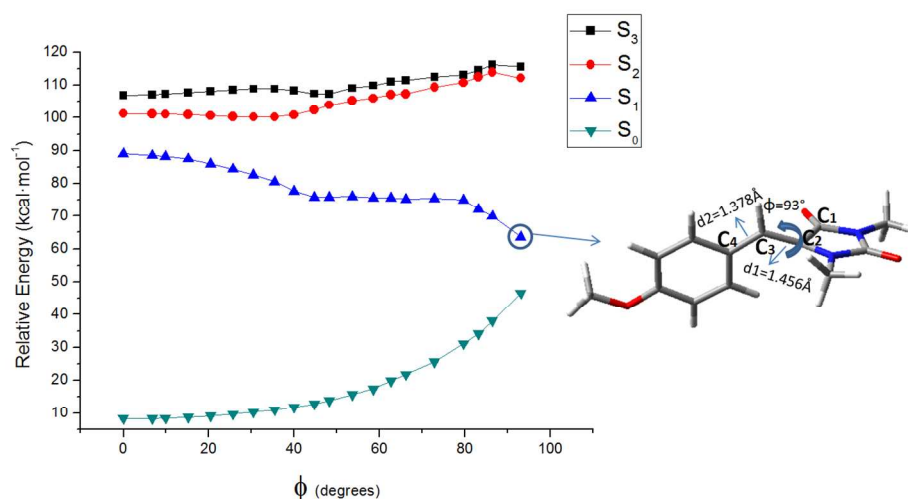


**Figure 11.** MS-CASPT2 single point energy corrections along the relaxation path on  $S_1$  computed at the CASSCF level of theory, as a function of the central double bond torsion coordinate ( $\phi$ ) for compound **7**. The structure of the final point is depicted.

From this point, the system can evolve in the ground state after radiative decay, recovering the *E* isomer or completing the photoisomerization reaching the *Z* isomer (Figure 12).

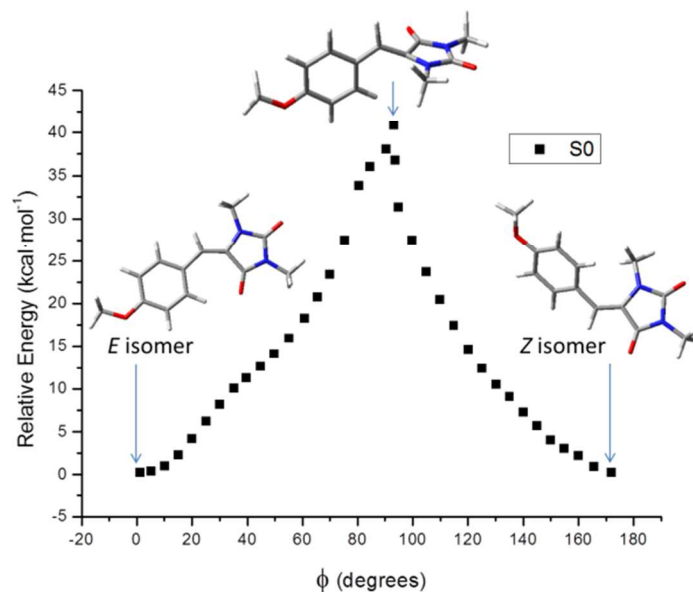


**Figure 12.** MS-CASPT2 single-point energy corrections along the minimum energy path on  $S_0$  from  $S_1$  minimum energy structure for **7** computed at the CASSCF level of theory.

Hence, the systems described herein comprise a novel family of efficient photoactive molecular switches as it has been verified computationally for one of its derivatives, **7**. Regarding the photophysical properties, the bright state is the first excited state ( $S_1$ ). Thus, crossings with other excited states that could deactivate the photoisomerization mechanism are avoided. Also, as no minimum was found in the excited state, no emission in the UV-Vis region is expected, confirming the experimental findings. Furthermore, these studies also confirm that the solvent effect in the absorption spectra of these systems is not large.

### 3. Conclusions

The synthesis and detailed photochemical studies of a new family of hydantoin based molecular photoswitches are presented. Although many applications of molecular switches have appeared in literature, most of them employ azobenzenes as the photoactive core. This family has shown an impressive potential once incorporated in complex systems, but the design of novel uses of switches requires the availability of diverse molecules with different properties. In this contribution we have established arylideneimidazolidine-2,4-diones as a new family of photoswitches: i) these compounds are very photostable, ii) in some cases, the switch can change completely between the *on /off* states, iii) the PSS can be controlled by external factors as the irradiation source or the filters used, iv) the light energy is used with high efficiency for the photoisomerization as no alternative pathways are available and v) easy to synthesize and amenable to scale up. In accordance, the mechanistic details obtained from the theoretical calculations allow to explain the experimental findings. Some of the future studies would be associated with modification of these compounds for specific applications. For example, biological applications of these photoswitches limited due to the absorption maxima in the UV region could be mitigated by affecting the absorption band through substitution, increasing the conjugation, including charges in the structure or through sensitized irradiation following already successful strategies for other switches.<sup>1,2,23</sup> Also, optical applications could be facilitated by affecting the gap

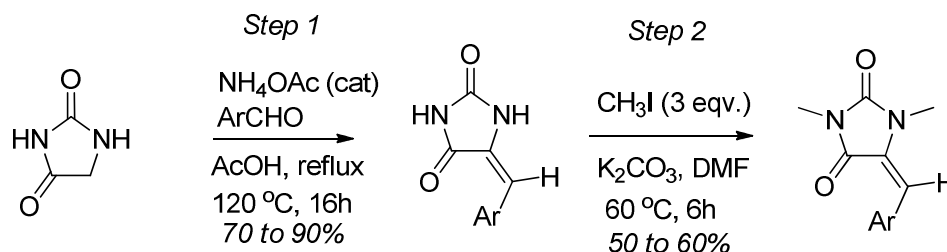
between the absorption bands for *E* and *Z* isomers and altering the PSS by careful choice of the wavelength of irradiation. In conclusion, arylideneimidazolidine-2,4-diones family consists of a significant extension of the molecular photoswitch concept. Further studies to include these molecules into complex systems are currently underway along with the design of new systems including 2-aminoimidazolones and pyrazolones.

#### 4. Experimental Section

**General Information.** All reactions were carried out in flame-dried glassware. Anhydrous solvents were purchased and used directly. Thin-layer chromatography (TLC) was carried out on precoated glass silica gel plates which were visualized with both ultraviolet light and stained with PMA.  $^1\text{H}$  and  $^{13}\text{C}$  NMR spectra were recorded on 400 MHz spectrometer. Chemical shifts are reported in ppm with reference to tetramethylsilane [ $^1\text{H}$ -NMR:  $\text{CDCl}_3$  (0.00  $\delta$ )] or solvent signals [ $^1\text{H}$ -NMR:  $\text{CDCl}_3$  (7.26  $\delta$ );  $^{13}\text{C}$ -NMR:  $\text{CDCl}_3$  (77.27  $\delta$ )]. Signal patterns are indicated as br (broad peak); s (singlet); d (doublet); t (triplet); q (quartet); m (multiplet). Infrared spectral data were obtained using a spectrometer with diamond ATR accessory as thin film. HRMS (TOF) data was obtained using ESI mode.

**Synthesis of arylideneimidazolidine-2,4-diones:** A series of arylideneimidazolidine-2,4-diones were prepared by following one of the two general methods described below.

##### Method 1:

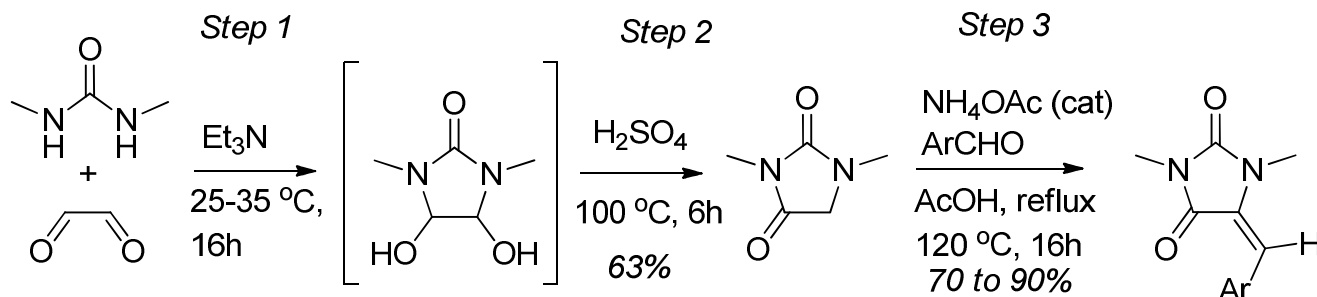


**Step 1:** A solution of imidazolidine-2,4-dione (2.16 g, 20 mmol) and ammonium acetate (276 mg, 3.6 mmol) in acetic acid (5 mL) was added to aldehyde (20 mmol) and the resulting mixture was stirred at

120 °C for 16 hours. After cooling, the reaction mixture was concentrated in vacuum and purified by column chromatography on silica gel with EtOAc-hexane to afford the 5-arylideneimidazolidine-2,4-diones (with yields ranging from 70 to 90%).

**Step 2:** To a solution of 5-arylideneimidazolidine-2,4-dione (20 mmol, 2.0 equiv) in dry DMF (50 mL) was added K<sub>2</sub>CO<sub>3</sub> (8.3 g, 60 mmol, 3.0 equiv) and methyl iodide (8.51 g, 60 mmol, 3 equiv). The resulting mixture was stirred for 12 h at 60 °C. The reaction was quenched by the addition of water. The resulting mixture was diluted with EtOAc (250 mL), and washed with water (50 ml x 3) and brine (100 ml). The organic layer was dried over anhydrous Na<sub>2</sub>SO<sub>4</sub>, filtered and concentrated. The resulting crude residue was purified by column chromatography on silica gel to give 5-arylidene 1,3-dimethylimidazolidine-2,4-diones in 50 to 60% yields.

### Method 2:



### Step 1:

A 1000 ml glass round-bottom flask equipped with a stirrer, thermometer and addition funnel was charged with 290 g (2.0 mol) of 40 wt % aqueous glyoxal solution and triethylamine (pH of the reaction mixture represented 9). Then, while maintaining the liquid temperature to 25 to 35 °C, a solution 1,3-dimethylurea (176 g (2.0 mol in 176 ml of water) was gradually added to the mixture. After addition was completed, the mixture was allowed to stir at the same temperature for 3 hours. After the completion of the reaction as monitored by TLC, the solvent was removed under reduced pressure on

rotavap to obtain 297 g of crude 4,5-dihydroxy-1,3-dimethyl-2-imidazolidinone as a colorless oil which was taken further for step 2 without further purification.

## Step 2

A 2000 ml glass round-bottom flask equipped with a stirrer, thermometer and a reflux condenser was loaded with 297 g of crude 4,5-dihydroxy-1,3-dimethyl-2-imidazolidinone prepared from the previous step, H<sub>2</sub>O (600 ml) and 98% sulfuric acid (54 g, 0.54 mol) and the resulting mixture was stirred for 6 hours at 95 °C to 100 °C. After completion of the reaction, the reaction mixture was cooled with an ice bath, and 90 g of sodium bicarbonate was added slowly. The crude residue was diluted with EtOAc/H<sub>2</sub>O (500 ml/200 ml). The aqueous layer was separated and extracted with EtOAc (100 ml x 3). The organic layers were combined and washed with brine (200 ml), dried over anhydrous Na<sub>2</sub>SO<sub>4</sub>, filtered and concentrated. The crude residue was purified by column chromatography on silica gel with EtOAc-hexane (20/80 to 35/65) to obtain 1,3-dimethylimidazolidin-2,4-dione as a colorless oil (161 g, 63% yield for two steps).

**<sup>1</sup>H-NMR** (400 MHz): 3.76 (2H, s), 2.87 (3H, s), 2.87 (3H, s); **<sup>13</sup>C-NMR** (100 MHz): 170.0, 157.0, 51.6, 29.5, 24.7; **IR**: 3444, 2949, 2358, 1760, 1699, 1493, 1419, 1388, 1272, 1248, 1110, 1077, 10005, 756, 599; **HR-MS** (ESI): calcd for C<sub>5</sub>H<sub>9</sub>N<sub>2</sub>O<sub>2</sub> [M+H]<sup>+</sup> 129.0664, found 129.0689.

**Step 3:** A solution of 1,3-dimethylimidazolidin-2,4-dione (2.56 g, 20 mmol) and ammonium acetate (276 mg, 3.6 mmol) in acetic acid (5 mL) was added to aldehyde (20 mmol) and the resulting mixture was stirred at 115 °C for 16 hours. After cooling, the mixture was concentrated in vacuum and purified either by recrystallization or by column chromatography on silica gel with EtOAc-hexane to afford the 5-arylideneimidazolidine-2,4-diones (with yields ranging from 70 to 90%).

Spectral data for various (*E*)-5-Arylidene-1,3-dimethylimidazolidine-2,4-diones obtained *via* the above methods are given below.



**(E)-5-(benzylidene)imidazolidine-2,4-dione (E-1):**

Yield = 2.63 g, 70 %  $^1\text{H-NMR}$  (300 MHz, DMSO- $d^6$ )  $\delta$  7.61 (d,  $J$  = 7.5 Hz, 2H), 7.40 (t,  $J$  = 7.4 Hz, 2H), 7.35 – 7.29 (m, 1H), 6.41 (s, 1H).  $^{13}\text{C-NMR}$  (300 MHz, DMSO)  $\delta$  165.6 (s), 155.7 (s), 133.0 (s), 129.4 (s), 128.8 (s), 128.4 (s), 128.0 (s), 108.3 (s). **UV-Vis** ( $\text{CH}_2\text{Cl}_2$  : MeOH):  $\lambda$  (nm) = 316 ( $\epsilon$ =20471  $\text{M}^{-1}\text{cm}^{-1}$ ), 331 ( $\epsilon$ = 16123  $\text{M}^{-1}\text{cm}^{-1}$ ). **EM-ES (+):** calcd for  $\text{C}_{10}\text{H}_8\text{N}_2\text{O}_2$   $[\text{M} + \text{H}]^+$  189.0664, found 189.0671. **Observations:** White solid.

**(Z)-5-(benzylidene)imidazolidine-2,4-dione (Z-1):**

$^1\text{H-NMR}$  (300 MHz, DMSO- $d^6$ )  $\delta$  ppm 7.89 (d,  $J$  = 7.3 Hz, 2H), 7.38 – 7.28 (m, 3H), 6.32 (s, 1H).  $^{13}\text{C-NMR}$  (300 MHz,  $\text{CDCl}_3$ )  $\delta$  163.6 (s), 153.9 (s), 133.1 (s), 129.9 (s), 128.1 (m), 115.6 (s). **UV-Vis** ( $\text{CH}_2\text{Cl}_2$  : MeOH):  $\lambda$  (nm) = 330 ( $\epsilon$ =13309  $\text{M}^{-1}\text{cm}^{-1}$ ). **EM-ES (+):** calcd for  $\text{C}_{10}\text{H}_8\text{N}_2\text{O}_2$   $[\text{M} + \text{H}]^+$  189.0664, found 189.0671. **Observations:** White solid.

**(E)-5-(4-nitrobenzylidene)imidazolidine-2,4-dione (E-2):**

Yield = 3.63 g, 78 %;  $^1\text{H-NMR}$ : (400 MHz, DMSO- $d^6$ )  $\delta$  ppm 8.19 (d,  $J$  = 8.4 Hz, 2H), 7.84 (d,  $J$  = 8.6 Hz, 2H), 6.49 (s, 1H).  $^{13}\text{C-NMR}$ : (100 MHz, DMSO- $d^6$ )  $\delta$  ppm 165.3 (s), 155.8 (s), 146.2 (s), 140.0 (s), 130.9 (s), 130.1 (s), 123.7 (s), 105.1 (s). **UV-Vis** ( $\text{CH}_2\text{Cl}_2$  : MeOH (1:1)):  $\lambda$  (nm) = 236 ( $\epsilon$ =8188  $\text{M}^{-1}\text{cm}^{-1}$ ), 353 ( $\epsilon$ = 15854  $\text{M}^{-1}\text{cm}^{-1}$ ) **EM-ES (+):** calcd for  $\text{C}_{10}\text{H}_8\text{N}_3\text{O}_4$   $[\text{M} + \text{H}]^+$  234.0515, found 234.0515. **Observations:** Brown solid.

**(E)-5-(2-hydroxybenzylidene)imidazolidine-2,4-dione (E-3):**

Yield = 3.06 g, 75 %;  $^1\text{H-NMR}$ : (400 MHz, DMSO- $d^6$ )  $\delta$  ppm 7.53 (d,  $J$  = 7.7 Hz, 1H), 7.15 (t,  $J$  = 7.9 Hz, 1H), 6.90 – 6.77 (m, 2H), 6.67 (s, 1H).  $^{13}\text{C-NMR}$ : (100 MHz, DMSO- $d^6$ )  $\delta$  ppm 165.7 (s), 156.0 (s), 155.5 (s), 130.0 (s), 129.5 (s), 127.2 (s), 120.1 (s), 119.4 (s), 115.6 (s), 104.0 (s). **UV-Vis** ( $\text{CH}_2\text{Cl}_2$  : MeOH (1:1)):  $\lambda$  (nm) = 235 ( $\epsilon$ =9800  $\text{M}^{-1}\text{cm}^{-1}$ ), 312 ( $\epsilon$ = 13200  $\text{M}^{-1}\text{cm}^{-1}$ ), 340 ( $\epsilon$  = 15200  $\text{M}^{-1}\text{cm}^{-1}$ ). **EM-ES (+):** calcd for  $\text{C}_{10}\text{H}_8\text{N}_2\text{O}_3$   $[\text{M} + \text{H}]^+$  205.0613, found 205.0615. **Observations:** White solid.

**(E)-5-((1H-indol-3-yl)methylene)imidazolidine-2,4-dione (E-4):**

Yield = 3.35 g, 74 % ; <sup>1</sup>H-NMR: (400 MHz, DMSO-d<sup>6</sup>) δ ppm 8.13 (s, 1H), 7.75 (d, *J* = 7.7 Hz, 1H), 7.42 (d, *J* = 7.7 Hz, 1H), 7.21-7.09 (m, 2H), 6.75 (s, 1H). <sup>13</sup>C-NMR: (100 MHz, DMSO) δ ppm 165.7 (s), 155.7 (s), 136.0 (s), 127.0 (s), 126.8(s), 123.8 (s), 122.6 (s), 120.4 (s), 118.2 (s), 112.1 (s), 108.6 (s), 102.1 (s). UV-Vis (CH<sub>2</sub>Cl<sub>2</sub> : MeOH (1:1)): λ (nm) =275 (ε=3602 M<sup>-1</sup>cm<sup>-1</sup>), 367 (ε=11835 M<sup>-1</sup>cm<sup>-1</sup>). EM-ES (+): calcd for C<sub>12</sub>H<sub>9</sub>N<sub>3</sub>O<sub>2</sub> [M+ H]<sup>+</sup> 228. 0773, found 228.0779. **Observations:** Orange solid.

**(E)-5-(3,5-dibromo-4-methoxybenzylidene)imidazolidine-2,4-dione (E-5):**

Yield = 5.71 g, 77 % <sup>1</sup>H-NMR: (300 MHz, DMSO-d<sup>6</sup>) δ ppm 8.09 (s, 2H), 5.59 (s, 1H), 3.76 (s, 3H). <sup>13</sup>C-NMR: (100 MHz, DMSO-d<sup>6</sup>) δ ppm 165.4 (s), 155.9 (s), 152.9 (s), 133.0 (s), 132.4 (s), 129.3 (s), 117.9 (s), 104.6 (s), 60.5 (s). UV-Vis (CH<sub>2</sub>Cl<sub>2</sub> : MeOH (1:1)): λ (nm) =321 (ε= 22605 M<sup>-1</sup>cm<sup>-1</sup>). EM-ES (+): calcd for C<sub>11</sub>H<sub>8</sub>Br<sub>2</sub>N<sub>2</sub>O<sub>3</sub> [M+ H]<sup>+</sup> 374.8980, found 374.8974. **Observations:** Brown solid.

**(Z)-5-(3,5-dibromo-4-methoxybenzylidene)imidazolidine-2,4-dione (Z-5):**

<sup>1</sup>H-NMR: (400 MHz, DMSO-d<sup>6</sup>) δ ppm 7.91 (s, 2H), 6.33 (s, 1H), 3.81 (s, 3H). <sup>13</sup>C-NMR: (100 MHz, DMSO-d<sup>6</sup>) δ ppm 165.20 (s), 155.7 (s), 153.0 (s), 133.0 (s), 132.1 (s) 129.1 (s), 117.9 (s), 104.5 (s), 60.5 (s). UV-Vis (CH<sub>2</sub>Cl<sub>2</sub> : MeOH (1:1)): λ (nm) =328 (ε= 14942 M<sup>-1</sup>cm<sup>-1</sup>), 342 (ε= 5747 M<sup>-1</sup>cm<sup>-1</sup>). EM-ES (+): calcd for C<sub>11</sub>H<sub>8</sub>Br<sub>2</sub>N<sub>2</sub>O<sub>3</sub> [M+ H]<sup>+</sup> 374.8980, found 374.8974. **Observations:** Brown solid.

**(E)-5-(benzylidene)-1,3-dimethylimidazolidine-2,4-dione (E-6):**

Yield = 3.51 g, 81 % <sup>1</sup>H NMR (300 MHz, CDCl<sub>3</sub>) δ ppm 7.41-7.28 (m, 5H), 6.95 (s, 1H), 3.14 (s, 3H), 2.95 (s, 3H). <sup>13</sup>C NMR (300 MHz, CDCl<sub>3</sub>) δ 163.7 (s), 155.8 (s), 132.6 (s), 129.6 (s), 129.4 (s), 128.3 (s), 128.2 (s), 112.2 (s), 30.5 (s), 24.9 (s). UV-Vis (CHCl<sub>3</sub>): λ (nm) =240 (ε= 7904 M<sup>-1</sup>cm<sup>-1</sup>), 309 (ε= 12316 M<sup>-1</sup>cm<sup>-1</sup>). EM-ES (+): calcd for C<sub>12</sub>H<sub>12</sub>N<sub>2</sub>O<sub>2</sub> [M+ H]<sup>+</sup> 217.0977, found 217.0972. **Observations:** Yellow oil.

**(E)-5-(4-methoxybenzylidene)-1,3-dimethylimidazolidine-2,4-dione (E-7):**

Yield = 3.95 g, 80 %; <sup>1</sup>H-NMR: (400 MHz, CD<sub>3</sub>CN) δ 7.96 (d, *J* = 8.9 Hz, 2H), 6.92 (d, *J* = 8.9 Hz, 2H), 6.28 (s, 1H), 3.81 (s, 3H), 3.12 (s, 3H), 2.98 (s, 3H). <sup>13</sup>C-NMR: (100 MHz, CD<sub>3</sub>CN) δ (ppm) 163.1

(s), 161.1 (s), 154.6 (s), 133.0 (s), 129.1 (s), 126.8 (s), 117.4 (s), 114.5 (s), 56.0 (s), 26.8 (s), 24.9 (s). **UV-Vis** (CHCl<sub>3</sub>):  $\lambda$  (nm) = 333 ( $\epsilon$  = 16346 M<sup>-1</sup>cm<sup>-1</sup>), 243 ( $\epsilon$  = 10115 M<sup>-1</sup>cm<sup>-1</sup>). **ES-MS (+)**: calcd for C<sub>13</sub>H<sub>14</sub>N<sub>2</sub>O<sub>3</sub> [M+ H]<sup>+</sup> 247.1083, found 247.1065. **Observations**: Yellow solid. CCDC-922962 contains the crystallographic data for this compound.

**(Z)-5-(4-methoxybenzylidene)-1,3-dimethylimidazolidine-2,4-dione (Z-7):**

**<sup>1</sup>H-NMR**: (400 MHz, CDCl<sub>3</sub>)  $\delta$  ppm 7.24 (d,  $J$  = 8.7 Hz, 2H), 6.93 (s, 1H), 6.90 (d,  $J$  = 3.8 Hz, 2H), 3.84 (s, 3H), 3.13 (s, 3H), 3.00 (s, 3H). **<sup>13</sup>C-NMR**: (100 MHz, CDCl<sub>3</sub>)  $\delta$  ppm 164.0 (s), 159.9 (s), 156.2 (s), 131.1 (s), 129.0 (s), 124.9 (s), 113.9 (s), 112.7 (s), 55.4 (s), 30.6 (s), 25.1 (s). **UV-Vis** (CHCl<sub>3</sub>):  $\lambda$  (nm) = 325 ( $\epsilon$  = 14808 M<sup>-1</sup>cm<sup>-1</sup>). **ES-MS (+)**: calcd for C<sub>13</sub>H<sub>14</sub>N<sub>2</sub>O<sub>3</sub> [M+ H]<sup>+</sup> 247.1083, found 247.1065. **Observations**: Yellow solid.

**(E)-5-(4-nitrobenzylidene)-1,3-dimethylimidazolidine-2,4-dione (E-8):**

Yield = 4.71 g, 90 % ; **<sup>1</sup>H-NMR** (300 MHz, CDCl<sub>3</sub>)  $\delta$  ppm 8.27 (d,  $J$  = 8.4 Hz, 2H), 7.47 (d,  $J$  = 8.5 Hz, 2H), 6.89 (s, 1H), 3.17 (s, 3H), 2.96 (s, 3H). **<sup>13</sup>C NMR** (400 MHz, CDCl<sub>3</sub>)  $\delta$  163.3 (s), 155.7 (s), 147.5 (s), 139.8 (s), 131.7 (s), 130.4 (s), 123.6 (s), 108.7 (s), 30.7 (s), 25.4 (s). **UV-Vis** (CHCl<sub>3</sub>):  $\lambda$  (nm) = 339 ( $\epsilon$  = 11816 M<sup>-1</sup>cm<sup>-1</sup>). **EM-ES (+)**: calcd for C<sub>12</sub>H<sub>11</sub>N<sub>3</sub>O<sub>4</sub> [M+ H]<sup>+</sup> 262.0828, found 262.0822. **Observations**: Orange solid.

**(E)-5-(2-methoxybenzylidene)-1,3-dimethylimidazolidine-2,4-dione (E-9):**

Yield = 3.91 g, 79% ; **<sup>1</sup>H NMR** (300 MHz, CDCl<sub>3</sub>)  $\delta$  ppm 7.34 (t,  $J$  = 7.4 Hz, 1H), 7.16 (d,  $J$  = 7.4 Hz, 1H), 7.02 – 6.88 (m, 3H), 3.85 (s, 3H), 3.13 (s, 3H), 2.94 (s, 3H). **<sup>13</sup>C NMR** (300 MHz, CDCl<sub>3</sub>)  $\delta$  163.6 (s), 157.6 (s), 155.8 (s), 130.7 (s), 130.0 (s), 129.9 (s), 121.5 (s), 119.9 (s), 110.4 (s), 108.8 (s), 55.4 (s), 29.8 (s), 4.9 (s). **UV-Vis** (CHCl<sub>3</sub>):  $\lambda$  (nm) = 242 ( $\epsilon$  = 10870 M<sup>-1</sup>cm<sup>-1</sup>), 326 ( $\epsilon$  = 12077 M<sup>-1</sup>cm<sup>-1</sup>). **EM-ES (+)**: calcd for C<sub>13</sub>H<sub>14</sub>N<sub>2</sub>O<sub>3</sub> [M+ H]<sup>+</sup> 247.1083, found 247.1077. **Observations**: Brown solid.

**(E)-5-((1-methyl-indol-3-yl)methylene)-1,3-dimethylimidazolidine-2,4-dione (E-10):**

Yield = 4.42 g, 82%; **<sup>1</sup>H NMR** (300 MHz, CDCl<sub>3</sub>)  $\delta$  ppm 7.68 (d,  $J$  = 8.0 Hz, 1H), 7.34 (t,  $J$  = 8.3 Hz, 2H), 7.24-7.19 (m, 1H), 7.15 (s, 1H), 7.10 (s, 1H), 3.85 (s, 3H), 3.17 (s, 3H), 3.15 (s, 3H). **<sup>13</sup>C NMR** (400 MHz, CDCl<sub>3</sub>)  $\delta$  164.2 (s), 156.4 (s), 136.8 (s), 129.8 (s), 128.4 (s), 127.5 (s), 123.0 (s), 120.8 (s),

119.7 (s), 109.93 (m), 107.7 (s), 106.0 (s), 33.3 (d,  $J = 15.0$  Hz), 30.2 (s), 25.1 (s). **UV-Vis** ( $\text{CHCl}_3$ ):  $\lambda$  (nm) = 373 ( $\epsilon = 13610 \text{ M}^{-1} \text{cm}^{-1}$ ). **EM-ES (+)**: calcd for  $\text{C}_{15}\text{H}_{15}\text{N}_3\text{O}_2$   $[\text{M} + \text{H}]^+$  270.1243, found 270.1242.

**Observations:** Brown solid.

**(*E*)-5-(3,5-dibromo-4-methoxybenzylidene)-1,3-dimethylimidazolidine-2,4-dione (*E*-11):**

Yield = 6.75 g, 84%;  $^1\text{H}$  NMR (400 MHz,  $\text{CDCl}_3$ )  $\delta$  ppm 7.44 (s, 2H), 6.72 (s, 1H), 3.92 (s, 3H), 3.14 (s, 3H), 3.00 (s, 3H).  $^{13}\text{C}$  NMR (300 MHz,  $\text{CDCl}_3$ )  $\delta$  163.4 (s), 155.8 (s), 154.3 (s), 133.5 (s), 131.4 (s), 131.0 (s), 118.2 (s), 108.2 (s), 61.0 (s), 30.8 (s), 25.3 (s). **UV-Vis** ( $\text{CHCl}_3$ ):  $\lambda$  (nm) = 316 ( $\epsilon = 8710 \text{ M}^{-1} \text{cm}^{-1}$ ). **EM-ES (+)**: calcd for  $\text{C}_{13}\text{H}_{12}\text{Br}_2\text{N}_2\text{O}_3$   $[\text{M} + \text{H}]^+$  402.9293, found 402.9282. **Observations:** Yellow solid.

**Typical procedure of irradiation:** The solutions of different photoswitches 1-5 in DMSO (0.01M) and 7-11 in  $\text{CDCl}_3$  (0.01M) were prepared and irradiated in separate NMR tubes using a 400 W medium-pressure Hg lamp until the PSS was reached. The reaction was followed by  $^1\text{H}$ -NMR. A similar procedure was followed with a light source centered at 350 nm. The solutions were placed in a merry-go-round appliance in a photoreactor and irradiated using lamps with emission wavelength centered at 350 nm (14 lamps x 8-W/ lamps) until the PSS was reached.

**Selective irradiation of the two isomers (*Z* and *E*) of 7:** The two isomers (*Z* and *E*) of compound 7 were irradiated separately with monochromatic light at different irradiation wavelengths: 300 nm, 330 nm and 375 nm. All the experiments were carried out under the same conditions with the same intensity of the monochromatic light.  $5.36 \times 10^{-5} \text{ M}$  solutions in dry acetonitrile were prepared. 3 ml of these solutions were irradiated at the selected wavelengths in a quartz cuvette (1.0 cm path length) using a monochromator until the PSS was reached. The photochemical reaction was followed by GC/MS.

**Isomerization quantum yield:** The isomerization quantum yield (photoswitch 4 or 7) was calculated following the procedure described in the literature, using *trans*-azobenzene as actinometer. First, a solution of *trans*-azobenzene in acetonitrile was prepared. The absorbance of this solution at 358 nm

was set to 1. Then, the actinometer solution was irradiated in a quartz cuvette at 334 nm using a monochromator. After a short period of time, the change in absorbance at 358 nm of was *ca.* 0.02. A solution in acetonitrile (for **7**) or CH<sub>2</sub>Cl<sub>2</sub>:MeOH 1:1 (for **4**) was prepared. The absorbance at 334 nm was adjusted to match the value of the actinometer. This solution was irradiated at 334 nm until a conversion of 20%. The isomerization process is followed by GC/MS. The number of photons absorbed by the sample was calculated by using the following formula:

$$E_p (\text{mol of photons} \times \text{cm}^{-2} \times \text{s}^{-1}) = F(\lambda) \times \Delta A (358\text{nm}) / t(\text{s})$$

where  $\Delta A(358\text{nm})$  is the change in the absorbance at 358 nm of the *trans*-azobenzene solution when irradiating at 334 nm, and  $t(\text{s})$  is the irradiation time responsible for that change. The F factor, which depends on the wavelength, has a value of  $3.6 \times 10^{-6}$  einstein  $\times \text{cm}^{-2}$  at 334 nm. Thus, the number of photons absorbed corresponds to  $E_p$  multiplied by the irradiation time (in seconds). The photochemical isomer formed after irradiating is quantified by GC/MS. The value for the isomerization quantum yield is obtained from the following equation:

$$\phi = \frac{\text{number of formed or destroyed molecules}}{\text{number of photons absorbed by the system}}$$

Finally, the actinometer solution was measured again to ensure that the light intensity is constant. All the solutions were kept in the dark during the whole experiment.

**Acknowledgments.** This research was supported by the Spanish Ministerio de Ciencia e Innovación (MICINN)/Fondos Europeos para el Desarrollo Regional (FEDER) (CTQ2011-24800 and CTQ2012-36966), and Project CCG2013/EXP-089 for the University of Alcalá (UAH). C.G.-I. thanks the Spanish MEC for her grant. S.R. acknowledges the support of National Science Foundation, USA (Grants no. CHE 1229339, and CHE1429086 for funds to purchase the 400 MHz NMR Spectrometer, and X-ray Diffractometer respectively).

**Supporting Information Available.** UV and luminescence data, NMR spectra, computational details and Cartesian coordinates for computed compounds. This material is available free of charge via the Internet at <http://pubs.acs.org>.

## References

- (1) Balzani, V.; Credi, A.; Venturi, M. *Molecular Devices and Machines: Concepts and Perspectives for the Nanoworld*; Wiley-VCH Verlag, Germany: Weinheim, 2008.
- (2) *Molecular Switches, 2nd Ed.*; Feringa, B. L.; Browne, W. R., Eds.; Wiley-VCH: Weinheim, 2011.
- (3) Bushuyev, O. S.; Tomberg, A.; Frišić, T.; Barrett, C. J. *J. Am. Chem. Soc.* **2013**, *135*, 12556.
- (4) Ritterson, R. S.; Kuchenbecker, K. M.; Michalik, M.; Kortemme, T. *J. Am. Chem. Soc.* **2013**, *135*, 12516.
- (5) Szymański, W.; Beierle, J. M.; Kistemaker, H. A. V.; Velema, W. A.; Feringa, B. L. *Chem. Rev.* **2013**, *113*, 6114.
- (6) Bogdavov, A.; Bobrovsky, A.; Ryabchun, A.; Vorobiev, A. *Phys. Rev. E* **2012**, *85*, 011704.
- (7) Mitchell, R. H. *Eur. J. Org. Chem.* **1999**, *1999*, 2695.
- (8) Muratsugu, S.; Kume, S.; Nishihara, H. *J. Am. Chem. Soc.* **2008**, *130*, 7204.
- (9) Roldan, D.; Kaliginedi, V.; Cobo, S.; Kolivoska, V.; Bucher, C.; Hong, W.; Royal, G.; Wandlowski, T. *J. Am. Chem. Soc.* **2013**, *135*, 5974.
- (10) Vilà, N.; Royal, G.; Loiseau, F.; Deronzier, A. *Inorg. Chem.* **2011**, *50*, 10581.
- (11) Irie, M. *Chem. Rev.* **2000**, *100*, 1685.
- (12) Irie, M.; Fukaminato, T.; Matsuda, K.; Kobatake, S. *Chem. Rev.* **2014**, *114*, 12174.
- (13) Tian, H.; Yang, S. *Chem. Soc. Rev.* **2004**, *33*, 85.
- (14) Ivashenko, O.; van Herpt, J. T.; Feringa, B. L.; Rudolf, P.; Browne, W. R. *Langmuir* **2013**, *29*, 4290.
- (15) Koçer, A.; Walko, M.; Meijberg, W.; Feringa, B. L. *Science* **2005**, *309*, 755.
- (16) Kohl-Landgraf, J.; Braun, M.; Özçoban, C.; Gonçalves, D. P. N.; Heckel, A.; Wachtveitl, J. *J. Am. Chem. Soc.* **2012**, *134*, 14070.
- (17) Lukyanov, B. S.; Lukyanova, M. B. *Chem. Heterocycl. Compd.* **2005**, *41*, 281.
- (18) Beharry, A. A.; Woolley, G. A. *Chem. Soc. Rev.* **2011**, *40*.
- (19) Samanta, S.; Woolley, G. A. *Chembiochem*, *12*, 1712.
- (20) Zarwell, S.; Ruck-Braun, K. *Tetrahedron Lett.* **2008**, *49*, 4020.
- (21) Feringa, B. L. *J. Org. Chem.* **2007**, *72*, 6635.
- (22) London, G.; Chen, K.-Y.; Carroll, G. T.; Feringa, B. L. *Chem. Eur. J.* **2013**, *19*, 10690.
- (23) Garcia-Iriepa, C.; Marazzi, M.; Frutos, L. M.; Sampedro, D. *RSC Advances* **2013**, *3*, 6241.
- (24) Blanco-Lomas, M.; Campos, P. J.; Sampedro, D. *Eur. J. Org. Chem.* **2012**, *2012*, 6328.
- (25) Blanco-Lomas, M.; Samanta, S.; Campos, P. J.; Woolley, G. A.; Sampedro, D. *J. Am. Chem. Soc.* **2012**, *134*, 6960.
- (26) Andruniow, T.; Fantacci, S.; De Angelis, F.; Ferre, N.; Olivucci, M. *Angew. Chem., Int. Ed.* **2005**, *44*, 6077.
- (27) Melloni, A.; Rossi Paccani, R.; Donati, D.; Zanirato, V.; Sinicropi, A.; Parisi, M. L.; Martin, E.; Ryazantsev, M.; Ding, W. J.; Frutos, L. M.; Basosi, R.; Fusi, S.; Latterini, L.; Ferré, N.; Olivucci, M. *J. Am. Chem. Soc.* **2010**, *132*, 9310.
- (28) Rivado-Casas, L.; Sampedro, D.; Campos, P. J.; Fusi, S.; Zanirato, V.; Olivucci, M. *J. Org. Chem.* **2009**, *74*, 4666.
- (29) Sinicropi, A.; Martin, E.; Ryasantsev, M.; Helbing, J.; Briand, J.; Sharma, D.; Léonard, J.; Haacke, S.; Canizzo, A.; Chergui, M.; Zanirato, V.; Fusi, S.; Santoro, F.; Basosi, R.; Ferré, N.; Olivucci, M. *Proc. Natl. Acad. Sci. USA* **2008**, *105*, 17642.
- (30) Blanco-Lomas, M.; Funes-Ardoiz, I.; Campos, P. J.; Sampedro, D. *Eur. J. Org. Chem.* **2013**, *2013*, 6611.

- (31) Funes-Ardoiz, I.; Blanco-Lomas, M.; Campos, P. J.; Sampedro, D. *Tetrahedron* **2013**, 69, 9766.
- (32) Cordes, T.; Elsner, C.; Herzog, T. T.; Hoppmann, C.; Schadendorf, T.; Summerer, W.; Rück-Braun, K.; Zinth, W. *Chem. Phys.* **2009**, 358, 103.
- (33) Cordes, T.; Schadendorf, T.; Rück-Braun, K.; Zinth, W. *Chem. Phys. Lett.* **2008**, 455, 197.
- (34) Cordes, T.; Weinrich, D.; Kempa, S.; Riesselmann, K.; Herre, S.; Hoppmann, C.; Rück-Braun, K.; Zinth, W. *Chem. Phys. Lett.* **2006**, 428, 167.
- (35) Regner, N.; Herzog, T. T.; Haiser, K.; Hoppmann, C.; Beyermann, M.; Sauermann, J.; Engelhard, M.; Cordes, T.; Rück-Braun, K.; Zinth, W. *J. Phys. Chem. B* **2012**, 116, 4181.
- (36) Schadendorf, T.; Hoppmann, C.; Rück-Braun, K. *Tetrahedron Lett.* **2007**, 48, 9044.
- (37) Steinle, W.; Rück-Braun, K. *Org. Lett.* **2002**, 5, 141.
- (38) Maerz, B.; Wiedbrauk, S.; Oesterling, S.; Samoylova, E.; Nenov, A.; Mayer, P.; de Vivie-Riedle, R.; Zinth, W.; Dube, H. *Chem. Eur. J.* **2014**, 20, 13984.
- (39) García-Iriepa, C.; Marazzi, M.; Zapata, F.; Valentini, A.; Sampedro, D.; Frutos, L. M. *J. Phys. Chem. Lett.* **2013**, 4, 1389.
- (40) Ruhemann, S.; Cunningham, A. *J. Chem. Soc.* **1899**, 75, 945.
- (41) Wheeler, H. L.; Hoffman, C. *Amer. Chem. J.* **1911**, 45, 368.
- (42) Anticancer: (a) Kaminsky, D. V.; Lesyk, R. B. *Biopolym. Cell* **2010**, 26, 136-145; (b) El-Deeb, I. M.; Bayoumi, S. M.; El-Sherbeny, M. A., *Eur. J. Med. Chem.* **2010**, 45, 2516-2530; Antibiotic: (c) J. Handzlik, E. Szymańska, S. Alibert, J. Chevalier, E. Otrębska, E. Pękala, J.-M. Pagès, K. Kieć-Kononowicz *Bioorg. Med. Chem.* **2013**, 21, 135-145; (d) J. Handzlik, A. Matys, K. Kieć-Kononowicz, *Antibiot.* **2013**, 2, 28-45; Antagonistic: (e) Handzlik, J.; Szymańska, E.; Wójcik, R. *Bioorg. Med. Chem.* **2012**, 20, 4245-4257.
- (43) Takano, S.; Kobayashi, T. *J. Soc. Cosmet. Chem. Jpn.* **1993**, 26, 262.
- (44) Blanco-Lomas, M.; Campos, P. J.; Sampedro, D. *Org. Lett.* **2012**, 14, 4334.
- (45) Tan, S. F.; Ang, K. P.; How, G. F. *J. Phys. Org. Chem.* **1990**, 3, 559.
- (46) Tan, S. F.; Ang, K. P.; How, G. F. *J. Phys. Org. Chem.* **1991**, 707.
- (47) Ware, E. *Chem. Rev.* **1950**, 46, 403.
- (48) Johnson, T. B.; Nicolet, B. H. *J. Am. Chem. Soc.* **1912**, 34, 1048.
- (49) In the setup used, the excitation spectrum was taken by moving the primary monochromator of the spectrofluorometer, while keeping fixed the reading wavelength of the secondary one. As these compounds feature very weak intensities, the slit in the secondary monochromator has to be wide open to read the emission pattern. Therefore the emission spectrum is obtained only for the registered absorption. The excitation spectrum shows the range of wavelengths which provide the emission spectrum. If this compound would have another emission band corresponding to a different excited state, we would get a different excitation band. Therefore the excitation spectrum may be the same as the absorption spectrum. In contrast, the absorption spectrum must contain the excitation spectra.
- (50) Kuhn, H. J.; Braslavsky, S. E.; Schmidt, R. *Pure Appl. Chem.* **2004**, 76, 2105.
- (51) Izquierdo-Serra, M.; Gascón-Moya, M.; Hirtz, J. J.; Pittolo, S.; Poskanzer, K. E.; Ferrer, È.; Alibés, R.; Busqué, F.; Yuste, R.; Hernando, J.; Gorostiza, P. *J. Am. Chem. Soc.* **2014**, 136, 8693.
- (52) *Computational Photochemistry*; Olivucci, M., Ed.; Elsevier: Amsterdam, 2005.
- (53) Sampedro, D. In *Photochemistry: UV/VIS Spectroscopy, Photochemical Reactions and Photosynthesis*; Maes, K. J., Willems, J. M., Eds.; Nova Science Publishers 2011.